Am J Transl Res 2023;15(7):4922-4931
www.ajtr.org /ISSN:1943-8141/AJTR0150652

Original Article

Network pharmacology of the Yigu Decoction empirical formula on the treatment of knee osteoarthritis

Jiaxin Wang[1], Chengyiye Ren[2], Yuepeng Xie[3]

[1]Zhejiang Chinese Medical University, Hangzhou 310000, Zhejiang, China; [2]Department of Pediatrics, Zhejiang Chinese Medicine University, Ningbo 315000, Zhejiang, China; [3]Department of Orthopedics and Traumatology, Third Affiliated Hospital of Zhejiang University of Traditional Chinese Medicine, Hangzhou 310000, Zhejiang, China

Received April 11, 2023; Accepted June 19, 2023; Epub July 15, 2023; Published July 30, 2023

Abstract: Objective: To investigate the mechanism of the Yigu Decoction empirical formula in the treatment of knee osteoarthritis (KOA) using network pharmacology and molecular docking methods. Methods: The active ingredients and targets of Yigu Decoction were screened using the TCMSP database. Relevant targets were predicted using several databases. A "drug-component-target-disease" network was constructed using Cytoscape software. A protein-protein interaction network was constructed using the STRING database. Gene Ontology and Kyoto Encyclopaedia of Genes and Genomes signalling pathways of the target genes were analysed. Results: We identified 18 components of Rhizoma drynariae (Gusuibu), 23 components of Yinyanghuo (*Herba Epimedii Brevicornus*), 16 components of Yam, 65 components of Danshen, 8 components of Sheng Di Huang (Rehmannia glutinosa), 29 components of Buguzhi (Psoralea corylifolia fruit), neoeriocitrin, and protocatechuic aldehyde. The targets were predicted using SwissTargetPrediction software. In total, 653 targets were screened, including 168 potential targets of Rhizoma drynariae (Gusuibu), 192 potential targets of Yinyanghuo (Herba Epimedii Brevicornus), 14 potential targets of Yam, 123 potential targets of Danshen, 216 potential targets of Sheng Di Huang (Rehmannia glutinosa), and 274 potential targets of Buguzhi (Psoralea corylifolia). Intersection analysis of a total of 2,292 targets related to KOA obtained from the GeneCard database, 30 targets from the OMIM database, 12 targets from the DrugBank database, and 368 targets from the DisGeNET database resulted in 2,316 target genes. Conclusions: Yigu Decoction can improve KOA through multiple targets and mechanisms. Yigu Decoction may be a useful alternative therapy for treating KOA.

Keywords: Knee osteoarthritis, Yigu Decoction, network pharmacology, molecular docking

Introduction

Knee osteoarthritis (KOA) is a metabolic bone disease characterised by subchondral bone growth and systemic mild inflammation. The prevalence of KOA is high among middle-aged and elderly women in China [1], leading to serious consequences of lifelong disability. The onset of KOA is unknown and most patients can only be diagnosed during physical examinations [2]. Current treatments include oral and topical nonsteroidal anti-inflammatory drugs (NSAIDs), tramadol, and topical capsaicin, which can alleviate the corresponding symptoms [3]. However, these drugs cause a series of side effects that cannot be ignored, such as increased risks of gastric ulcer and subcutaneous mucosal bleeding. Therefore, safer and more effective preventive strategies are needed.

Traditional Chinese Medicines (TCMs) have a long history of use to prevent and treat KOA. KOA belongs to the categories of "involving the bone" and "bone atrophy". Many TCMs have been used to safely and effectively treat KOA [4, 5]. Yigu Decoction (YGD) is a clinical prescription comprised of Psoralea corylifolia, Rhizoma Drynariae, Herba Epimedii, Radix Rehmanniae, Radix Salviae Miltiorrhizae, and Rhizoma Dio0 scoreae that has been demonstrated to invigorate the kidney and activate blood circulation. The specific mechanism of YGD in treating KOA remains unclear, and the components and key targets have yet to be determined, given the complex components, multiple targets, and wide levels of TCM compounds.

Based on the theory of system biology, network pharmacology uses big data for network analysis, selects disease target genes and active ingredients of TCM compounds, designs multi-target drug molecules, and systematically and comprehensively studies the interaction between "drug-target-pathway-disease" [6]. This concept is consistent with the holistic view of TCM and the principle of treatment based on syndrome differentiation. In this study, we used network pharmacology to analyse the activity of YGD and predict its potential targets and signalling pathways. The findings provide new ideas for the study of KOA and the mechanism of action of YGD in treating KOA.

Data source and methods

Chemical component collection and target prediction of YGD

The active ingredients of Boneset, Epimedium, Yam, and Salvia were retrieved using the Traditional Chinese Medicine Systems Pharmacology Database and Analysis Platform (TCMSP) database (https://tcmsp-e.com/) [7]. An oral bioavailability (OB) ≥ 30% and drug-likeness (DL) ≥ 0.18 were the criteria to screen the active ingredients. The chemical components of Radix et Rhizoma and Radix Psoralen were searched using the Batman database using a score ≥ 20 to screen the components. The collated targets were calibrated using UniProt (https://www.uniprot.org/) data to obtain the standardized gene names.

Acquisition of targets related to KOA

The keyword "Knee osteoarthritis" was entered into the GeneCards (https://www.genecards.org/), OMIM (https://omim.org/), and DisGeNET (https://omim.org/) databases to obtain targets related to KOA. To improve the feasibility of the results, targets with "M (marker/mechanism)" or "T (therapeutic)" markers in the Comparative Toxicogenomics Database (CTD) [8], targets with Score_gda ≥ 0.01 in the DisGeNET database [9], and targets with Relevance score ≥ 5 in GeneCards [10] were selected. The targets obtained from each database were combined and de-duplicated to finally filter out KOA-related disease targets. Drugs registered through the Food and Drug Administration (FDA) for KOA were searched in DRUGBANK (https://go.drugbank.com) [11] to obtain their drug therapeutic targets. All targets from the four databases were integrated into Excel software and duplicate genes were excluded, followed by correction using the UniProt database.

Drug-disease target prediction results

The targets of ingredients were mapped to the targets of KOA. Venn plots were generated to obtain the intersection genes. Cytoscape 3.8.2 software was used to construct the "compound-target" network. A greater value for the degree, closeness centrality (CC), and betweenness centrality of a node indicated higher relevance of a node to the network. Thus, the core components were selected.

Protein-protein interaction (PPI) network construction

The drug-interacting genes were uploaded to the STRING database (https://string-db.org/) for PPI generation. The species was set to "Homo sapiens" and the minimum interaction score was set to 0.9 to ensure the reliability of the study. The remaining parameters were kept as default. The TSV file was uploaded into Cytoscape 3.8.2 and the network was analysed (Cytoscape→Tools→Network analyser→Network analysis→Analyse network). Node size and colour were used to reflect the degree of size, with larger node indicating larger degree value. The thickness of the edge was used to reflect the comfort score, with a thicker edge indicating larger combine score. The core targets were used to plot a PPI network.

Gene Ontology (GO) enrichment and Kyoto Encyclopaedia of Genes and Genomes (KEGG) pathway analyses

The DAVID database (https://david.ncifcrf.gov/summary.jsp) [12] was used for GO enrichment analysis. The gene identifier was selected as OFFICIAL_GENE_SYMBOL, and the species was set as Homo sapiens. Using DAVID 6.8, the role of target proteins in the gene function of YGD for KOA was annotated by BP, CC, and MF, and KEGG pathway enrichment analysis was performed to elucidate the pathways enriched by targets of YGD for KOA.

Molecular docking experiments

The three-dimensional structure of the small molecule was downloaded in sdf format from

Figure 1. Veen diagram of drug-disease intersection targets. It shows 221 drug-disease intersection genes between the targets of compounds related to Yigu Decoction and the targets related to KOA. YGD, Yigu Decoction; KOA, knee osteoarthritis.

the PubChem database and imported into ChemBio3D Ultra 14.0 for energy minimisation. The Minimum RMS Gradient was set to 0.001, and the small molecules were saved in the mol2 format. The optimised small molecule was imported into AutodockTools-1.5.6 for hydrogenation, charge calculation, charge assignment, and rotatable key setting, and saved as the "pdbqt" format.

The key targets and components were selected from the PPI and component-target networks for molecular docking. Key target proteins (human-derived proteins with high structural similarity between the original ligands and the active ingredients to be docked, and high resolution) were downloaded from the Protein Data Bank database (http://www.rcsb.org/). Pymol 2.3.0 was used to remove protein crystalline water, and raw ligands.

AutoDock Vina1.1.2 was used for docking (parameters are provided in the Supplementary Material). Small molecules with the best scores were selected for interaction pattern analysis, and the docking results were analysed using PyMOL 2.3.0 and LIGPLOT V 2.2.4.

Results

Prediction of active ingredients and targets of YGD

Eighteen components of Rhizoma drynariae (Gusuibu), 23 components of Yinyanghuo (Herba Epimedii Brevicornus), 16 components of Yam, 65 components of Danshen, 8 components of Sheng Di Huang (Rehmannia glutinosa), 29 components of Buguzhi (Psoralea corylifolia fruit), neoeriocitrin, and protocatechuic aldehyde were identified. The targets were predicted using the SwissTargetPrediction software. In total, 653 targets were screened, including 168 potential targets of Rhizoma drynariae (Gusuibu), 192 potential targets of Yinyanghuo (Herba Epimedii Brevicornus), 14 potential targets of Yam, 123 potential targets of Danshen, 216 potential targets of Sheng Di Huang (Rehmannia glutinosa), and 274 potential targets of Buguzhi (Psoralea corylifolia). All data are provided in the Supplementary Tables 1, 2.

Targets related to KOA

A total of 2,292 targets related to KOA were downloaded from the GeneCards database, including 30 from the OMIM database, 368 from the DisGeNET database, and 12 from the DrugBank database. The data from the four databases were intersected. Using the GeneCards database as the standard, duplicate genes were removed using Excel, and finally 2,316 target genes were obtained, which were corrected using the UniProt database. All data are provided in the Supplementary Table 3.

Drug-disease target prediction results

We identified 221 drug-disease intersection genes between the targets of compounds related to YGD and the targets related to KOA (**Figure 1**). Cytoscape 3.8.2 was used to construct the "ingredient-target" network, and the key ingredients were screened by Cytohubba. The key ingredients were kaempferol, luteolin, quercetin, bakuchiol, stigmasterol backuchiol, angelicin, and gamma-aminobutyric acid. These may be the major effective compounds in the treatment of KOA (**Figure 2**).

Core targets and network interactions

The 221 shared targets obtained from the Venn diagram of the component targets of YGD and the targets of KOA were imported into the STRING database for PPI prediction, with species set to Homo sapiens and confidence level set to 0.9. The network file was saved in the TSV format, which was then imported into

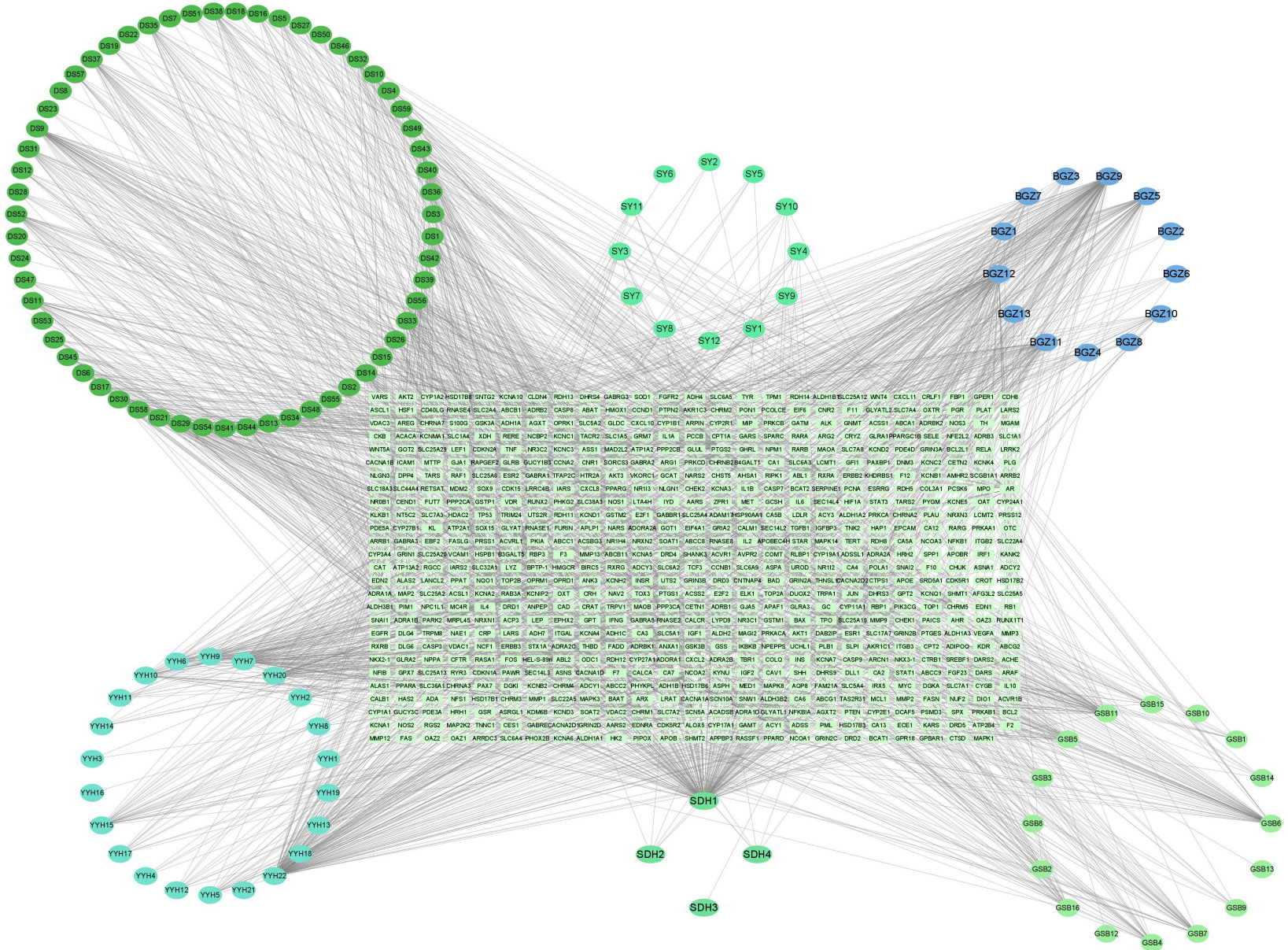

Figure 2. Key component-target network diagram. String and Cytoscape were used to screen the key targets. Network of the key ingredients and the targets in YGD for the treatment of KOA. YGD, Yigu Decoction; KOA, knee osteoarthritis.

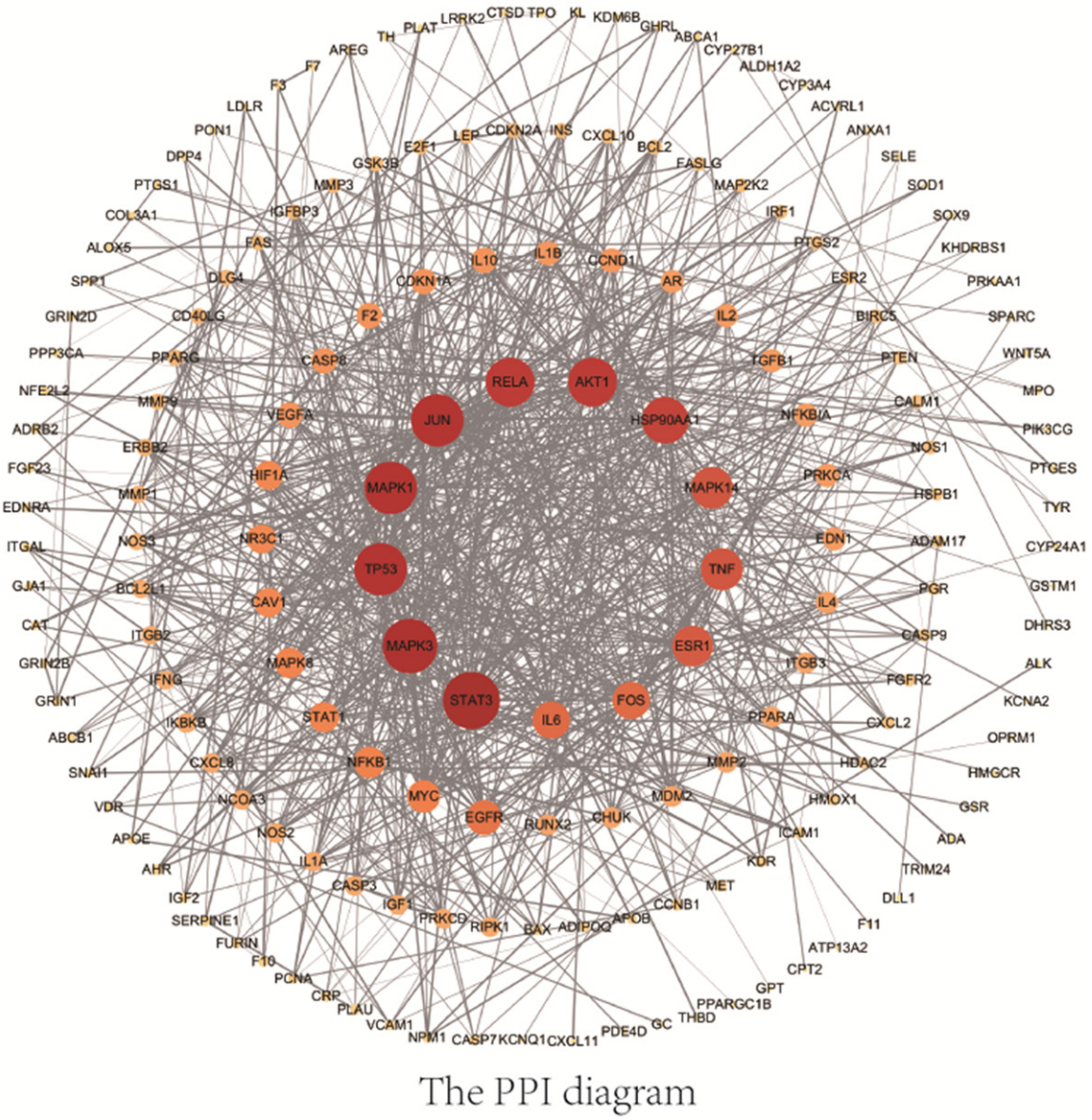

The PPI diagram

Figure 3. Protein-protein interaction (PPI) network diagram.

Cytoscape 3.8.2 software to draw the PPI network. Topological analysis of the network was performed. The degree value is reflected by the size and colour of the target points, and the combined score value is reflected by the thickness of the edges used to construct the PPI network (**Figure 3**). The network had 176 nodes and 839 edges. The parameters related to the core target network with the top 20-degree values are listed in **Table 1**.

Functional enrichment analysis

GO enrichment analysis: A total of 1,039 GO entries were screened using the DAVID database for GO enrichment analysis. Of the total entries, 815 were related to BP. Thirty major entries significantly enriched were screened out using $P < 0.05$ as the criterion (**Figure 4A**). The processes mainly involved signal transduction, apoptotic process, cell proliferation, inflammatory response, positive regulation of gene expression, apoptotic process, lipopolysaccharide response, negative regulation of cell proliferation, and redox process. Ninety-two entries were related to CC and involved plasma membrane, cytoplasm, nucleus, cytosol, mitochondria, and others. One hundred thirty-two entries were related to MF and involved protein binding, enzyme binding, aden-

Table 1. Parameters related to the core target network

Gene	Protein name	Freedom	Closeness Centrality	Betweenness Centrality
STAT3	RAC-alpha serine/threonine-protein kinase	45	0.48	0.09
MAPK3	Mitogen-activated protein kinase	43	0.50	0.07
MAPK1	Mitogen-activated protein kinase 1	41	0.49	0.06
JUN	Transcription factor AP-1	41	0.47	0.05
TP53	Cellular tumor antigen p53	41	0.47	0.10
AKT1	RAC-alpha serine/threonine-protein kinase	38	0.48	0.08
RELA	Transcription factor p65	38	0.47	0.04
HSP90AA1	Heat Shock Protein 90 Alpha Family Class A Member 1	36	0.47	0.06
TNF	Tumor necrosis factor	32	0.45	0.04
MAPK14	Mitogen-activated protein kinase 14	32	0.46	0.06
ESR1	Estrogen receptor	31	0.46	0.06
IL6	Interleukin 6	28	0.42	0.02
FOS	Proto-oncogene c-Fos	28	0.44	0.03
EGFR	Epidermal growth factor receptor	26	0.45	0.04
MYC	Myc proto-oncogene protein	24	0.45	0.02
NFKB1	Nuclear factor NF-kappa-B p105 subunit	23	0.43	0.02
STAT1	Signal transducer and activator of transcription 1-alpha/beta	22	0.43	0.01
MAPK8	Mitogen-activated protein kinase 8	22	0.41	0.03
HIF1A	Hypoxia-inducible factor 1-alpha	21	0.43	0.01
NR3C1	Glucocorticoid receptor	21	0.44	0.02

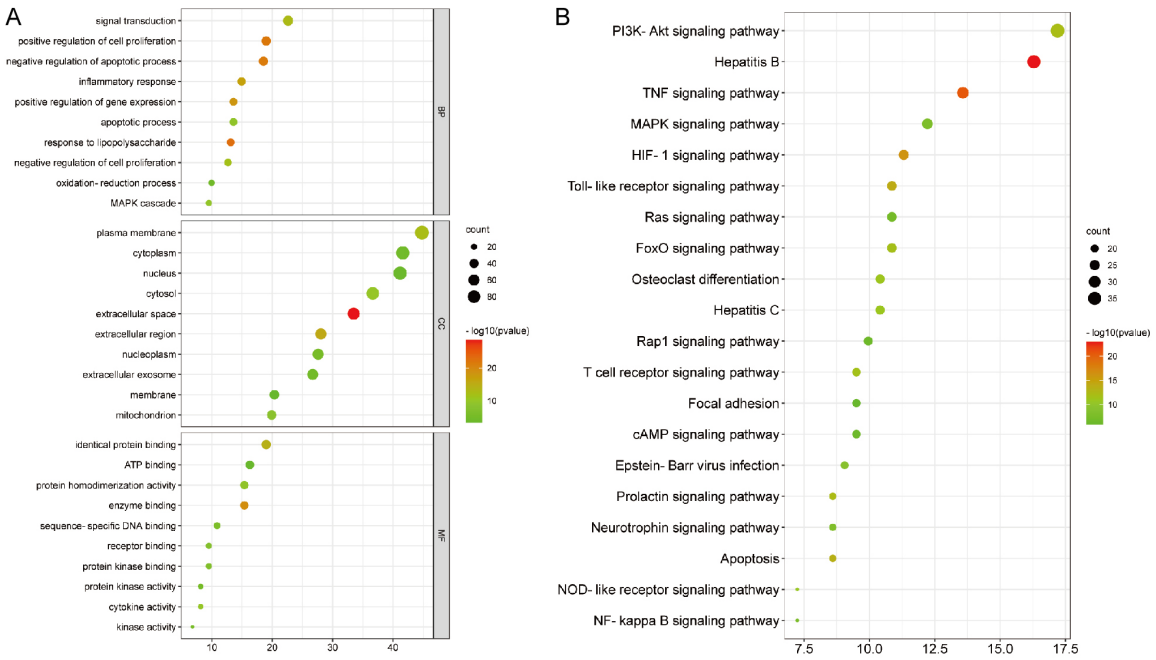

Figure 4. Results of functional enrichment analysis. A. Gene Ontology; B. Kyoto Encyclopedia of Genes and Genomes (KEGG) analysis (top 20) (Based on the *P*-values, the top 20 KEGG metabolic pathways were selected. A bubble chart was drawn based on the *P*-values, with the horizontal axis representing the number of genes enriched in the pathway. The size of the bubble represents the number of genes enriched in the corresponding pathway, and the depth of the colour represents significance. Significantly enriched information can be intuitively observed).

osine triphosphate binding, zinc ion binding, transcription factor binding, receptor binding, sequence-specific DNA binding, and others.

KEGG pathway enrichment analysis: A total of 137 pathways related to the treatment of KOA with YGD were enriched ($P < 0.05$). The most significantly enriched pathways were phosphoinositide 3-kinase-protein kinase B (PI3K-AKT) signalling, tumour necrosis factor (TNF) signalling, mitogen-activated protein kinase (MAPK) signalling, hypoxia-inducible factor-1 (HIF-1) signalling, osteoclast differentiation, cAMP signalling, T-cell receptor signalling, Toll-like receptor (TLR) signalling, neurotrophin signalling, and apoptosis. The top 20 KEGG pathways were filtered according to the *P*-value, and a bubble plot was drawn according to the *P*-value (**Figure 4B**).

Molecular docking results

AKT1-stigmasterol: The binding energy of stigmasterol with AKT1 was -7.3 kcal/mol, indicating a binding interaction. Stigmasterol interacted with AKT1 mainly through the formation of hydrogen bonds as well as hydrophobic forces, forming hydrogen bonds with Glu91 (A) with a hydrogen bond length of 2.94 Å, which showed hydrophobic interactions with His13 (A), Trp11 (A), Glu40 (A), Leu12 (A), Pro24 (A), Glu95 (A), and Val90 (A) (**Figure 5A**).

Heat shock protein 90kDa alpha (cytosolic), member A1 (HSP90AA1)-luteolin: The binding energy of luteolin with HSP90AA1 was -9.3 kcal/mol, indicating a good binding interaction. Luteolin interacted with HSP90AA1 with only hydrophobic interaction force between the two, which showed hydrophobic interactions with Leu48 (A), Ser52 (A), Met98 (A), Val186 (A), Leu107 (A), Tyr139 (A), Asp93 (A), Phe138 (A), and Asn51 (A) (**Figure 5B**).

JUN-stigmasterol: The binding energy of stigmasterol with JUN was -6.9 kcal/mol, indicating a good binding effect. Stigmasterol interacted with JUN with only hydrophobic forces between the two, showing hydrophobic interactions with Lys285 (B), Val284 (B), Lys283 (B), Leu280 (A), Arg279 (A), and Glu281 (B) (**Figure 5C**).

MAPK3-stigmasterol: The binding energy of stigmasterol to MAPK3 was -9.5 kcal/mol, demonstrating a strong binding relationship. Stigmasterol interacted with MAPK3, with only hydrophobic forces between the two, which showed hydrophobic interactions with Asp123 (A), Asn171 (A), Tyr53 (A), Thr127 (A), Met125 (A), Ile48 (A), Ala69 (A), Leu173 (A), Leu124 (A), Val56 (A), Cys183 (A), Ser170 (A), Glu50 (A), and Asp184 (A) (**Figure 5D**).

RELA-kaempferol: The binding energy of kaempferol with RELA was -7.4 kcal/mol, indicating a good binding interaction. Kaempferol interacted with RELA mainly through the formation of hydrogen bonds as well as hydrophobic forces, forming hydrogen bonds with His170 (B) with a length of 3.08 Å, which showed hydrophobic interactions with Leu186 (B), Gln185 (B), Leu173 (B), Leu176 (B), Cys159 (B), Gly166 (B), Val169 (B), Leu193 (B), Asp172 (B), Glu190 (B), Arg184 (B) (**Figure 5E**).

MAPK1-kaempferol: The binding energy of kaempferol with MAPK1 was -9.1 kcal/mol, indicating a good binding interaction. Kaempferol interacted with MAPK1, mainly through the formation of hydrogen bonds as well as hydrophobic forces with Met108 (A) and Lys54 (A), with hydrogen bond lengths of 3.02 Å and 2.81 Å, respectively; it showed hydrophobic interactions with Leu107 (A), Ala52 (A), Leu156 (A), Asp167 (A), Gly34 (A), Asp111 (A), Ser153 (A), Ile31 (A) (**Figure 5F**).

STAT3-stigmasterol: The binding energy of stigmasterol with STAT3 was -7.6 kcal/mol, demonstrating good binding. Stigmasterol interacted with STAT3 mainly via the formation of hydrogen bonds and hydrophobic forces, forming hydrogen bonds with Asp334 (A) with a hydrogen bond length of 2.97 Å, which showed hydrophobic interactions with Arg335 (A), His332 (A), Pro471 (A), Val563 (A), Glu616 (A), Asn567 (A), Asp566 (A), and Asp570 (A) (**Figure 5G**).

TP53-luteolin: The binding energy of luteolin with TP53 was -7.1 kcal/mol, demonstrating good binding. luteolin interacted with TP53 mainly via the formation of hydrogen bonds and hydrophobic forces with His115 (A), Asn131 (A), Gln104 (A), with hydrogen bond lengths of 3.01 Å, 2.95 Å, 3.14 Å, which showed hydrophobic interactions with Phe113 (A), Tyr126 (A), Asp268 (A), Arg110 (A), Leu111 (A), Gly112 (A) (**Figure 5H**).

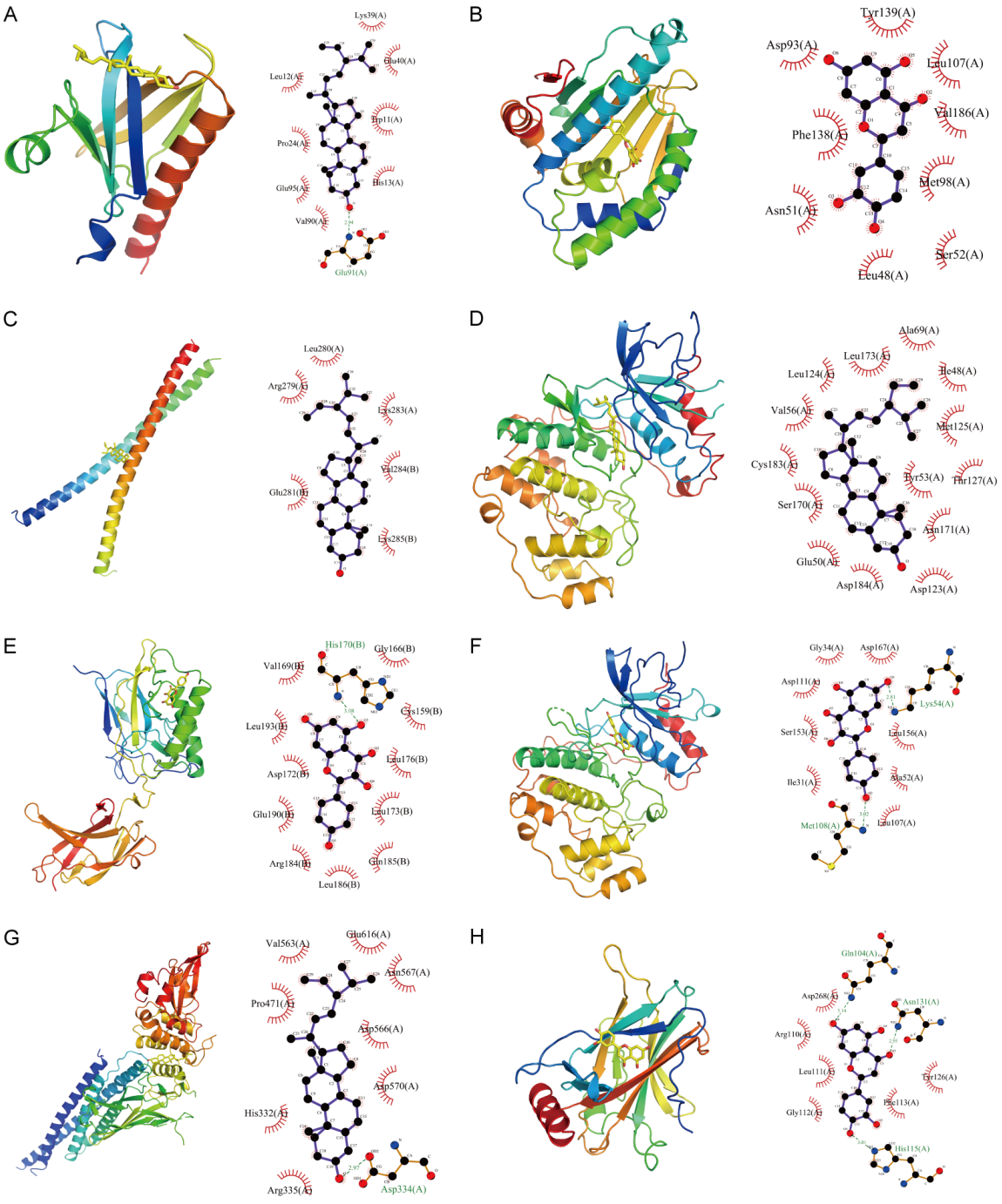

Figure 5. Results of molecular docking. A. AKT1-stigmasterol. B. (HSP90AA1)-luteolin. C. JUN-stigmasterol. D. MAPK3-stigmasterol. E. RELA-kaempferol. F. MAPK1-kaempferol. G. STAT3-stigmasterol. H. TP53-luteolin.

Discussion

YGD is a clinical formula proposed by Prof. Yao Xinmiao for the treatment of Guwei bone diseases based on the unique theory of "Tonify kidney and promote blood circulation" combined with "deficiency followed by atrophy". KOA belongs to the TCM categories of "Guwei" and "Gubi", which have highly similar disease typologies. The efficacy of YGD for blood stasis in KOA due to Qi stagnation category is promising. Network pharmacology evidence indicates that YGD can interfere with KOA through several signalling pathways, including the PI3K-AKT,

TNF, MAPK, HIF-1, T-cell receptor, and neurotrophic pathways, osteoclast differentiation, cAMP signalling, TLR signalling, and apoptosis. The pathways are mostly involved in energy metabolism and immune response and other biological processes. Among them, MAPK1, MAPK3, and MAPK14 are critical molecules in the MAPK signalling pathway [13], which is the common intersection pathway of cell proliferation [14], stress, inflammation, differentiation, functional synchronization, transformation [15], and apoptosis. These proteins are involved in cell proliferation, differentiation, carcinogenesis, metastasis, and apoptosis. Multiple effects can be produced by different growth and stress stimuli in different cells via diverse signalling pathways confined by alternative cytoskeletons [15]. However, a clearer explanation is still needed for the therapeutic effect of YGD on KOA. Therefore, we conducted network pharmacology and molecular docking experiments to indicate the direction for future *in vitro* and *in vivo* experiments.

In this study, the active ingredients, targets, molecular pathways, and biological processes of YGD in the treatment of KOA were studied and analysed using network pharmacology. A total of 161 active ingredients of botanicals and 653 targets of compounds in the YGD were screened using the TCMSP database, as well as Batman analysis and literature evidence. The screening identified 221 potential therapeutic targets. Six main components of YGD and their compounds for the effective treatment of KOA were screened out, and KEGG and GO results suggest that there are multiple pathways for YGD intervention in KOA, suggesting that the mechanism of YGD in treating KOA is complex, and YGD has multiple therapeutic targets for KOA.

The existing KOA therapeutic targets were obtained from the DrugBank database. We compared 221 results with drugs used in the treatment of KOA which are registered on the FDA (https://www.fda.gov/). There were 12 common targets between YGD and the six drugs registered in the FDA, including diclofenac, diclofenac, duloxetine, aminoglucose, hyaluronic acid, and zucapsaicin (a topical analgesic). The mechanisms of these drugs include inhibiting secretion of cyclooxygenase-1 and -2 in OA (diacerein and diclofenac) [16], suppressing pain (duloxetine, zucapsaicin) [17, 18], protecting cartilage and promoting cartilage regeneration (aminoglucose, hyaluronic acid) [19, 20], and reducing nerve impulses and nerve sensitivity associated with OA pain (hyaluronic acid) [20].

In summary, potential targets, biological processes, and signalling pathways of YGD in treating osteoporosis were predicted using network pharmacology, and its mechanism of action in treating osteoporosis is revealed. The findings will provide a reference and basis for performing relevant biological experiments in the future. It will be necessary to effectively integrate basic research with targets and construct a complete disease network. However, this study lacks experimental evidence. Further organisation and analysis of the data need to be improved. In addition, molecular docking has not been able to retrieve all options.

Acknowledgements

This study was funded by the project of Intervention of Wenshen Huoxue Prescription on Cartilage Injury in Degenerative Knee Osteoarthritis (project code: 2019XJ08) (21ZQ-048).

Disclosure of conflict of interest

None.

Address correspondence to: Yuepeng Xie, Department of Orthopedics and Traumatology, Third Affiliated Hospital of Zhejiang University of Traditional Chinese Medicine, Hangzhou 310000, Zhejiang, China. Tel: +86-15279102596; E-mail: xypeng0410@yeah.net

References

[1] Tang X, Wang S, Zhan S, Niu J, Tao K, Zhang Y and Lin J. The prevalence of symptomatic knee osteoarthritis in China: results from the China health and retirement longitudinal study. Arthritis Rheumatol 2016; 68: 648-653.

[2] Mahmoudian A, Lohmander LS, Mobasheri A, Englund M and Luyten FP. Early-stage symptomatic osteoarthritis of the knee - time for action. Nat Rev Rheumatol 2021; 17: 621-632.

[3] Hochberg MC, Altman RD, April KT, Benkhalti M, Guyatt G, McGowan J, Towheed T, Welch V, Wells G and Tugwell P; American College of Rheumatology. American College of Rheumatology 2012 recommendations for the use of nonpharmacologic and pharmacologic thera-

pies in osteoarthritis of the hand, hip, and knee. Arthritis Care Res (Hoboken) 2012; 64: 465-474.
[4] Hao Y, Wu Y, Wang S, Wang C, Qu S, Li L, Yu G, Liu Z, Zhao Z, Fan P, Zhang Z and Shi Y. Quantitative proteomics reveal the protective effects of EDS against osteoarthritis via attenuating inflammation and modulating immune response. J Ethnopharmacol 2021; 271: 113780.
[5] Luo Y, Zhang Y and Huang Y. Icariin reduces cartilage degeneration in a mouse model of osteoarthritis and is associated with the changes in expression of Indian hedgehog and parathyroid hormone-related protein. Med Sci Monit 2018; 24: 6695-6706.
[6] Chen L, Chu C, Lu J, Kong X, Huang T and Cai YD. Gene ontology and KEGG pathway enrichment analysis of a drug target-based classification system. PLoS One 2015; 10: e0126492.
[7] Ru J, Li P, Wang J, Zhou W, Li B, Huang C, Li P, Guo Z, Tao W, Yang Y, Xu X, Li Y, Wang Y and Yang L. TCMSP: a database of systems pharmacology for drug discovery from herbal medicines. J Cheminform 2014; 6: 13.
[8] Davis AP, Grondin CJ, Johnson RJ, Sciaky D, Wiegers J, Wiegers TC and Mattingly CJ. Comparative toxicogenomics database (CTD): update 2021. Nucleic Acids Res 2021; 49: D1138-D1143.
[9] Piñero J, Ramírez-Anguita JM, Saüch-Pitarch J, Ronzano F, Centeno E, Sanz F and Furlong LI. The DisGeNET knowledge platform for disease genomics: 2019 update. Nucleic Acids Res 2020; 48: D845-D855.
[10] Safran M, Dalah I, Alexander J, Rosen N, Iny Stein T, Shmoish M, Nativ N, Bahir I, Doniger T, Krug H, Sirota-Madi A, Olender T, Golan Y, Stelzer G, Harel A and Lancet D. GeneCards version 3: the human gene integrator. Database (Oxford) 2010; 2010: baq020.
[11] Wishart DS, Feunang YD, Guo AC, Lo EJ, Marcu A, Grant JR, Sajed T, Johnson D, Li C, Sayeeda Z, Assempour N, Iynkkaran I, Liu Y, Maciejewski A, Gale N, Wilson A, Chin L, Cummings R, Le D, Pon A, Knox C and Wilson M. DrugBank 5.0: a major update to the DrugBank database for 2018. Nucleic Acids Res 2018; 46: D1074-D1082.
[12] Dennis G Jr, Sherman BT, Hosack DA, Yang J, Gao W, Lane HC and Lempicki RA. DAVID: database for annotation, visualization, and integrated discovery. Genome Biol 2003; 4: P3.
[13] Hirota Y, Yamashita S, Kurihara Y, Jin X, Aihara M, Saigusa T, Kang D and Kanki T. Mitophagy is primarily due to alternative autophagy and requires the MAPK1 and MAPK14 signaling pathways. Autophagy 2015; 11: 332-343.
[14] Zhang W and Liu HT. MAPK signal pathways in the regulation of cell proliferation in mammalian cells. Cell Res 2002; 12: 9-18.
[15] Cipriano R, Miskimen KL, Bryson BL, Foy CR, Bartel CA and Jackson MW. FAM83B-mediated activation of PI3K/AKT and MAPK signaling cooperates to promote epithelial cell transformation and resistance to targeted therapies. Oncotarget 2013; 4: 729-738.
[16] Gan TJ. Diclofenac: an update on its mechanism of action and safety profile. Curr Med Res Opin 2010; 26: 1715-1731.
[17] Sałat K, Jakubowska A and Kulig K. Zucapsaicin for the treatment of neuropathic pain. Expert Opin Investig Drugs 2014; 23: 1433-1440.
[18] Petersen KK, Drewes AM, Olesen AE, Ammitzbøll N, Bertoli D, Brock C and Arendt-Nielsen L. The effect of duloxetine on mechanistic pain profiles, cognitive factors and clinical pain in patients with painful knee osteoarthritis-A randomized, double-blind, placebo-controlled, crossover study. Eur J Pain 2022; 26: 1650-1664.
[19] Yuan PW, Yu HC, Zhou HZ, Zhu C, Qu Q and Liu DY. Preventive administration of juanbi capsules for knee osteoarthritis: effects on serum MMP-2 and MMP-9 levels and cartilage repair. J Tradit Chin Med 2011; 31: 334-337.
[20] Moreland LW. Intra-articular hyaluronan (hyaluronic acid) and hylans for the treatment of osteoarthritis: mechanisms of action. Arthritis Res Ther 2003; 5: 54-67.